KfK 4563
April 1989

Ion Beam Modification and Analysis of Thin $YBa_2Cu_3O_7$ Films

O. Meyer
Institut für Nukleare Festkörperphysik

Kernforschungszentrum Karlsruhe

KERNFORSCHUNGSZENTRUM KARLSRUHE

Institut für Nukleare Festkörperphysik

KfK 4563

ION BEAM MODIFICATION AND ANALYSIS OF THIN $YBa_2Cu_3O_7$ FILMS

O. Meyer

Kernforschungszentrum Karlsruhe GmbH, Karlsruhe

Kernforschungszentrum Karlsruhe GmbH
Postfach 3640, 7500 Karlsruhe 1

ISSN 0303-4003

ABSTRACT

The application of ion beams for the analysis and modification of high Tc superconductors is reviewed. Ion backscattering and channeling spectroscopy is used to optimize the film composition and the epitaxial growth performance on various single crystalline substrates. The influence of radiation damage on the transport properties and on the structure of polycrystalline as well as of single crystalline thin films is presented. The irradiation induced metal to insulator phase transition is discussed in detail. Some applications including the use of ion implantation for structuring are summarized.

Anwendung von Ionenstrahlen zur Analyse und zur Modifikation von einkristallinen Hoch-T_c Schichten

ZUSAMMENFASSUNG

Es wird über den Einsatz von Ionenstrahlen mit Energien im Bereich von 0.3 bis 3.5 MeV bei der Herstellung und Modifikation von dünnen Filmen des Hoch-Tc-Supraleiters $YBa_2Cu_3O_7$ berichtet. Die Ionen-Rückstreu- und Channeling-Spektroskopie wird erfolgreich eingesetzt bei der Optimierung der Zusammensetzung und bei der Analyse des epitaxialen Wachstums der Schichten auf verschiedenen einkristallinen Substratmaterialien. Weiterhin wird der Einfluß der Strahlenschädigung auf die Transporteigenschaften und die Struktur der Schichten dargestellt. Insbesondere werden Untersuchungen zum bestrahlungsinduzierten Metall-Isolator Phasenübergang beschrieben, und es werden einige Anwendungen der Ionenimplantation wie z.B. zur Strukturierung von Hoch-T_c Schichten behandelt.

INTRODUCTION

There has been a continuous interest in irradiation experiments of superconductors like A15 and Chevrel phases or refractory carbides and nitrides from both the scientific and applied points of view. The knowledge of the degradation of the superconducting transition temperature, T_c, by irradiation induced defects is of importance if superconductors are applied in a radiation environment. On the other hand defects which may act as pinning centers have been introduced into superconductors to improve such properties like the critical current. (For a review see ref. [1]).

It is well known that the superconducting properties of materials are strongly affected by chemical and structural disorder. Thus from a more basic point of view it is important to know the correlations between T_c depression and defect structures with other, e.g. transport properties, which can provide information on the microscopic parameters which in a given class of superconductors are important for high T_c achievement. Particle irradiation is often used to produce intrinsic damage in a controllable fashion in order to study the influence of disorder on the superconducting properties in a wide damage concentration, ranging up to levels where phase transformations, e.g. amorphization, occur. Previously, the change of the critical temperature, T_c, as a function of the radiation induced increase of the residual resistivity, $\Delta\rho_0$, revealed in general a universal behaviour depending on whether the Fermi level, E_F, was located either in a peak or a valley of the electronic density of states (DOS). Lattice defects lead to a lifetime broadening of electronic states and thus to a smearing of the peaks in the DOS. Under the assumption that the electron-phonon coupling constant, λ, was proportional to the density of states at E_F, T_c was calculated as a function of $\Delta\rho_0$ [2].

The structure of the defects causing large changes of T_c in A15 superconductors has been studied by TEM, X-ray diffraction and by Rutherford backscattering and channeling spectroscopy. The T_c decrease of high-T_c A15 superconductors is usually correlated with the decrease of the Bragg-Williams long-range order parameter S, i.e. with the formation of antisite defects by irradiation [3] or by deviations in composition from stoichiometry [4]. More recently it has been shown for Nb_3Ir that both, T_c increase and T_c decrease with increasing ion fluence are accompanied by a decrease of S[5] . Further, the

changes of T_c are accompanied by a defect structure consisting of static displacements of the lattice atoms with average rms amplitudes of 0.005 to 0.009 nm, which can be interpreted as a static Debye Waller factor [6,7] . Both the depressions and enhancements in T_c have been explained by changes in the electronic density of states at the Fermi energy $N(E_F)$ due to smearing effects. The elastic properties of V_3Si and Nb_3Ir are also strongly affected by particle irradiation leading to a large defect-induced stiffening of the average shear elastic constant for V_3Si [8] , while for Nb_3Ir a large softening of this long-wave length shear mode is observed [9] . In both cases the changes of the elastic constants are again correlated with the changes of $N(E_F)$ and of T_c, correspondingly.

In comparison with the former superconductors, the high-T_c oxide superconductors have a rather low DOS at E_F and it is well known that by lowering the oxygen concentration $N(E_F)$ can be reduced [10] and a transition from the orthorhombic metallic phase to the tetragonal semiconducting phase can easily be enforced [e.g. 11,12] . The oxygen atoms are rather mobile and diffuse even near room temperature [13] . Thus it is concievable that oxygen atoms which are displaced during irradiation can strongly change the electronic properties of these oxides. A universal behaviour between T_c depression and resistivity increase cannot be expected due to such competing phase transitions. Numerous irradiation studies have already been performed using electrons [14,15,16] ions [17-27] and neutrons [28,29,30] . In general, a rapid decrease of T_c, a considerable broadening of the transition width, δT_c, and large increase of the residual resistivity, ρ_o, with increasing particle fluence is observed. Although large differences are noted concerning the T_c dependence on the deposited energy density during irradition, there is a general agreement that the oxides range in their sensitivity scale to radiation damage between the Chevrel phases and the A15 superconductors. The origin for the observed T_c depression is still under debate. From electron irradition experiments it was concluded that the decrease of T_c is mainly due to point defects (bulk effect) while from n-irradiation results it was concluded that the superconducting properties are mainly affected by intragrain radiation damage. Intragrain radiation damage was directly seen as amorphous zones on the grain boundaries by transmission electron microscopy [20] . The differences in the radiation sensitivity of various oxide materials can be attributed to the material quality ranging from loosely coupled intergrain material to single-crystalline quality with quite different initial values of T_c, δT_c and resistivity ρ. For example a dramatic loss of the

superconductivity was observed by irradiating plasma-arc sprayed films with low fluences ($< 10^{14}$ cm^{-2}) of H and He ions [26] . Therefore it seems to be important to separate bulk effects from intergrain effects on the changes of the superconducting properties upon irradiation.

In the following the influence of radiation damage on the electronic transport properties and the structure of polycrystalline, highly textured as well as large area single crystalline thin film is presented. Due to the strong dependences of the irradiation effects on the material quality it is necessary to characterize the thin films in great detail. Thus the preparation and the ion beam analysis concerning structure and properties of the films used for the irradiation experiments are described in the first chapter. In the second chapter the effects of ion irradiation on T_c , δT_c and ρ are described considering the initial film properties as parameter. The irradiation induced metal-semiconductor transition is presented in detail. Defect structure analyses by TEM, X-ray diffraction and high energy (2-3 MeV) He-ion channeling will be discussed. Some applications including the use of ion implantation are summarized in the last chapter.

1. Thin Film Synthesis and Analysis

Thin films have provided valuable information on the superconducting properties. Highly textured and epitaxial films exhibited critical transport currents well above 1 x 10^6 A/cm^2 at 77 K [31] , far larger than those measured for bulk samples ($\sim 10^3$ A/cm^2) or single crystalline bulk samples [32] . A variety of thin film deposition techniques has been used up to now to produce thin films with T_c-onset values similar to those obtained for bulk samples. Among these techniques are r.f. sputtering [18,33,34] , a.c.-sputtering [35] and d.c. sputtering [36] from composite targets as well as d.c.-magnetron sputtering from multi-targets [37] . Electron beam evaporation from multiple sources has been used to produce thin films [38,39] as well as molecular beam epitaxy [40] . Other techniques such as pulsed laser evaporation of bulk material [41] , and screen printing [42] have also been successfully applied.

1.1 Thin Film Preparation

In order to obtain high quality films it is necessary not only to have the correct composition but to perform a proper annealing treatment in oxygen and to avoid chemical reactions with the substrate. Thus the choice of the substrate

material and of the deposition process plays an important role, and the reproducible preparation of high quality high-T_c oxide superconductors in thin film form on desired substrates is still a problem of considerable challenge.

Most of the deposition techniques use a 3-step process: (a) Highly disordered or amorphous material with the stoichiometric composition is deposited at substrate temperatures up to 500°C. (b) The films are then transformed into the tetragonal phase at about 900°C in 1 atm. oxygen (O_2) and (c) are finally converted into the orthorhombic high-T_c phase by annealing the tetragonal phase in O_2 at temperatures below 600°C. The phase transformation at 900°C causes considerable interface reactions with various substrates such as Al_2O_3, MgO, ZrO_2 and $SrTiO_3$ [42,43,44] . Thus the quality of the films deposited in a three step procedure with thicknesses below 0.5 μm is rather limited. Further the nucleation of the crystalline films does not only occur at the film /substrate interface but may occur as well at the surface or at appropriate nucleation centers within the highly disordered film. Therefore the growth of a large area single crystalline high-T_c oxide film is strongly limited.

Recently a 2-step process was developed using a planar type magnetron sputter gun where the highly crystalline tetragonal phase could successfully be deposited at substrate temperatures of 800°C and below [34,45,46,46a] . Due to these substantially lower substrate temperatures interface reactions could considerably be suppressed and the quality of the films becomes independent of the film thickness for thicknesses above 0.1 μm and independent of various substrate materials used. Using this technique, thin superconducting films with the nominal composition $YBa_2Cu_3O_7$ have been deposited by magnetron sputtering from a composite target on (100)-$SrTiO_3$ substrates at 800°C and were heated in situ at 430°C in pure O_2 atmosphere. Details of the deposition process are described in Ref. [45] . The gas pressure in the discharge was 2×10^{-1} Torr O_2 and 4×10^{-1} Torr Ar. A cathode voltage of 100 Volts and a current of 0.5 A was used. The substrates were placed 20-30 mm apart from the target on a Pt-stripe which could be resistively heated up to 1100°C. The deposition rate was typically 5 Å/s. The deposition process was further improved using a hollow cathode type magnetron gun [46] . The film composition was examined by Rutherford backscattering with 2 Mev $^4He^+$ ions.

Backscattering spectrometry is a well-known analysis technique for thin films [47] . For the development of the sputter guns this technique has successfully

been applied in routine analysis of numberless thin films in order to optimize the many parameters of the sputtering process and the annealing procedures. The resonant scattering of 3.04 MeV He-ions on O has been used to enhance the detection sensitivity for oxygen. Further, the epitaxial growth of these films is analyzed using high energy ion backscattering combined with channeling. This allows the analyses of intrinsic defect structures or of defects produced by ion irradiation. The advantages of ion channeling for interface and epitaxial growth analysis are described in detail elsewhere [48]. In brief, variations of compositions at interfaces due to reactions can be analyzed nondestructively together with the crystalline quality of the deposited film as a function of depth. Lattice mismatch and the associated strain can be determined as well as the extent of mosaic spread (misorientation of the crystallites with respect to the substrate orientation) and the occurrence of special defect structures e.g. dislocations within the film.

As an example the yield of 2 MeV He-ions, backscattered from Y-Ba-Cu-O thin films which were deposited onto Al_2O_3 at different substrate temperatures is shown in Fig 1. The channel numbers can be converted in a mass scale and in a depth scale. It can be seen that the yields from Ba, Y, Cu and Al (from the underlying substrates) are well separated, especially for the film deposited at 760°C. From the corresponding step heights, the relative composition of Cu, Y and Ba can be determined. From the changes of the step heights with increasing substrate temperature it can be evaluated that the Ba/Y-ratio increases from about 1.7 to 3.5 with T_s increasing from 760°C to 870°C reaching the stoichiometric ratio at 820°C. Further it is noted that the composition profile near the interface deteriorates with increasing T_s.This could be due to either interface reactions or due to large variations of the film thickness as observed for island growth [49]. Sputter Auger experiments which also indicate interface diffusion [46a] will have similar problems in profile evaluation if the films are inhomogeneous in thickness or contain pinholes.

1.2 Epitaxial Growth and Intrinsic Defects

The two-step process was well suited to grow single crystalline $YBa_2Cu_3O_7$ films on (100) and (110)-$SrTiO_3$ substrates. The growth has been studied by ion channeling spectroscopy [50,50a] and X-ray diffraction [51] and it was shown

that the substrate temperature and the substrate orientation are important parameters. On (110) substrate films grow either in the (110) or in the mixed (110)/(013) direction. On (100) substrates c-axis orientation is observed at elevated temperatures (Ts ≃ 780-830°C)while a-axis orientation occurs at lower temperatures ($T_s < 720°C$) [51].

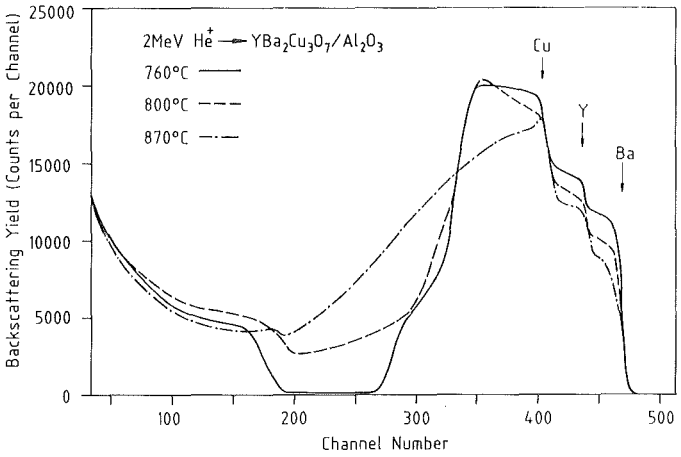

Fig.1 Backscattering spectra of $YBa_2Cu_3O_7$ thin films sputtered onto Al_2O_3 substrates at various substrate temperatures.

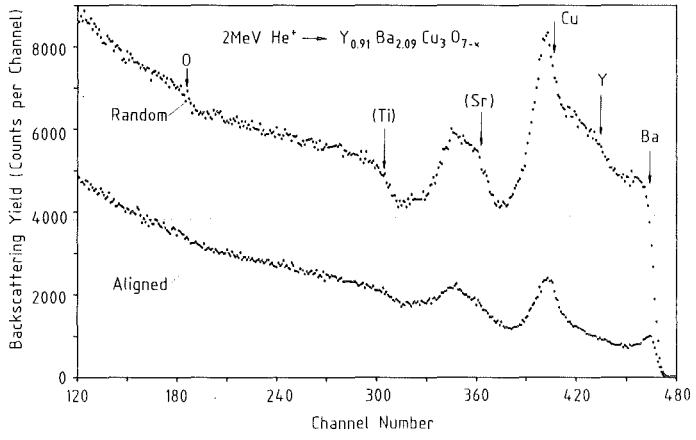

Fig. 2 Random and <100> aligned backscattering spectra from YBaCuO thin films sputtered on (100) $SrTiO_3$ (analyzing He ion beam energy is 2.0 MeV).

The growth of the films in the single crystalline phase has also been analyzed by channeling experiments. Fig. 2 shows the random and (100)-aligned backscattering spectra of 2 MeV He ions of a single crystalline $YBa_2Cu_3O_7$ film grown on $SrTiO_3$. The front edges of the various components in the film and the substrate are indicated by arrows. The Cu-yield is overlapped with the Sr-yield which in turn together with the Ti-yield is shifted to lower energies as the He-

particles have to penetrate the $YBa_2Cu_3O_7$ film in order to reach the substrate. From the step heights of the random spectrum a composition of $Y_{0.91}Ba_{2.09}Cu_3O_{7-x}$ can be determined. From the ratio of the (100)-aligned yield to the random yield behind the surface peak ($\approx$channel 450) a relative minimum yield value, X_{min} for Ba of 16% is obtained. This is considerably better than values observed previously for films deposited by molecular beam epitaxy [40] and pulsed laser evaporation [41] where the films have been annealed at high temperatures after deposition. It clearly shows that the transformation from the disordered into the tetragonal phase at about 900°C does not exclusively start at the film/substrate interface. This represents a severe disadvantage of the 3 step preparation method. It has been shown previously that the minimum yield values decrease with decreasing analyzing beam energy which indicates that mainly dislocations contribute to the backscattered yield of the aligned spectra [50] . These dislocations could act as pinning centers as will be discussed below.

A further question is concerned with the quality of the epitaxial growth, especially the misorientation of the $YBa_2Cu_3O_7$ crystallites with respect to the $SrTiO_3$ crystal orientation. Ion channeling is a very sensitive technique to explore this problem [48] . In this case the Ba-yield is measured as a function of the angle between the incident He ion beam and the crystal orientation. The result of such a measurement is shown in Fig. 3 and is called angular yield curve. The angular yield curve is defined by the critical angle, $\Psi_{1/2}$ which is the half angle at half height between the random yield and the minimum yield,[48] . The channeling process can be evaluated in more detail by performing Monte Carlo simulation calculations through the various crystal directions in well defined tilt planes. The one-dimensional vibration amplitudes used for this calculation were 0.083 Å for Ba, 0.076 Å for Y, an averaged value of 0.067 Å for Cu(1) and Cu(2) and an averaged value of 0.088 Å for O(1), O(2), O(3) and O(4). These values are all based on high resolution neutron diffraction measurements [52] . The results of such a calculation in c-direction for the Ba- and Y-yield choosing a tilt plane 15 degrees off the (100) plane is also shown in Fig. 3 (solid line). The calculated values of 0.88° for Ba and 0.92° for Y are in rather good agreement with the measured values. In the a- or b-directions the calculated values are 0.87° and 0.75° for the Ba and Y rows, respectively. These data clearly show that the c axis of the deposited film consisting of Ba_2Y rows with similar steering force for Ba and Y is perpendicular to the substrate surface. This result is supported by the RHEED small angle diffraction pattern [50] and by X-ray diffraction [51]. As the analyzing beam of about 1 mm^2 averages over thousands of crystallites it is

reasonable to assume a Gaussian distribution of the crystallite orientations with a standard deviation σ. Convoluting the calculated angular yield curve for Ba with a Gaussian curve (σ = 0.25°), the result represented by the solid line in Fig. 3 is observed. As can be seen the measured results can be simulated rather well using σ = 0.25° and random contribution to the yield of 12% due to scattering from dislocations.

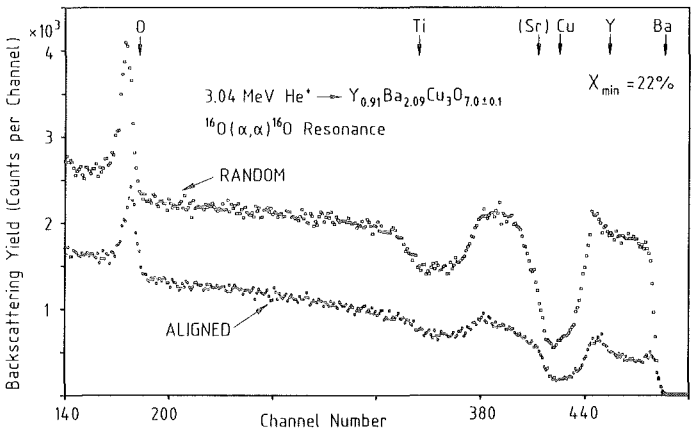

Fig. 3 Random and <100> aligned backscattering spectra from $Y_{0.91}Ba_{2.09}Cu_3O_{7.0}$ thin films sputtered on (100)$SrTiO_3$ (analyzing He ion energy is 3.04 MeV).

The superconducting properties of thin films are not only determined by the composition and the defect structures present but especially by the amount and the lattice location of the oxygen. For bulk samples usually thermogravimetric methods are successfully used to determine the oxygen content. For thin films nuclear reactions or the resonant enhanced scattering cross section may be used to get some information about the oxygen concentration and the lattice location of oxygen. In Fig. 4 the random and <100>-aligned backscattering spectra are shown for a $YBa_2Cu_3O_7$ thin film on $SrTiO_3$ using an incident He-ion energy of 3.04 MeV. The contributions of the various components in the film and the substrate are indicated by arrows.The yield from oxygen is now strongly enhanced and can be used to determine the relative concentration of oxygen. The sensitivity enhancement factor (SEF) of 16 has been obtained from a similar analysis of $SrTiO_3$ with stoichiometric composition [50] . From the peak area of the oxygen resonance peak for the random spectrum in Fig. 4, together with the SEF-factor of 16 as deter- mined above from the analysis of $SrTiO_3$, a relative composition of $Y_{0.91}Ba_{2.09}Cu_3O_{7.0 \pm 0.1}$ was obtained for this film.

Prior to deposition, the (100) $SrTiO_3$ substrates were analyzed by ion channeling and backscattering and the influence of various surface preparation

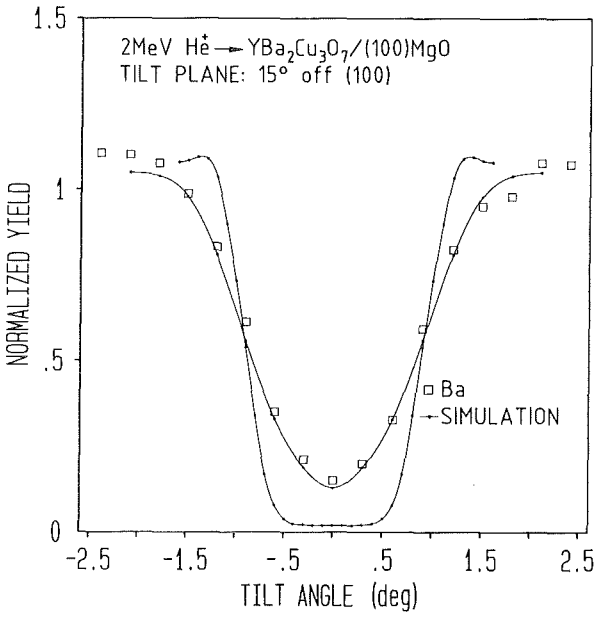

Fig. 4 Angular scan through the <100> axial direction of a $YBa_2Cu_3O_7$ thin film. The angular yield curve for Ba is shown together with the calculated angular yield curve of a perfect crystal. The latter curve is modified to fit the experimental values (solid line) assuming a mosaic spread of 0.25° and a displaced atom fraction of 12%.

techniques such as polishing, etching, sputtering and annealing in 1 atm O_2 was studied [50]. $SrTiO_3$ single crystalline substrates obtained from different manufactorers revealed quite different crystalline quality. The minimum yield values, varied between 1.5% and 30%. The dechanneling yield as a function of depth indicated that high minimum yield values were mainly due to high densities of partial dislocations throughout the bulk region. Some $SrTiO_3$ single crystals were of excellent quality as was checked by measuring and analyzing the surface peak areas of Sr and Ti in the aligned backscattering spectra of (100) $SrTiO_3$. The results compared with Monte Carlo calculations indicated that a nearly perfect (100) $SrTiO_3$ surface could be obtained by ion etching followed by annealing in O_2. Similar results have been obtained for highly polished and annealed $SrTiO_3$ surfaces. The results clearly show that a perfect substrate surface is a necessary precondition for good epitaxial growth of $YBa_2Cu_3O_7$ film on (100) $SrTiO_3$.

1.3 Thin Film Properties

The superconducting transition temperatures were determined by AC-susceptibility measurements and by the resistive method using 4 point contacts of Al-stripes connected to the films by silver paste. DC currents of 1-100 μA were applied for these measurements. As the films were found to be laterally homogeneous over typical distances of 15 mm the current and voltage contacts

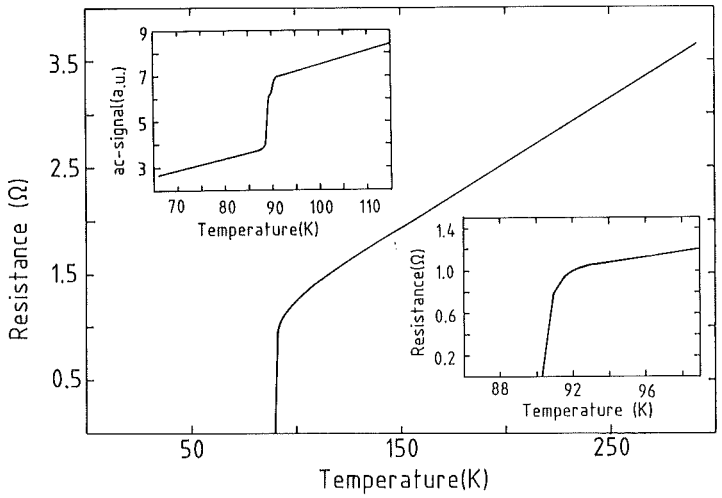

Fig. 5. Superconducting transition temperature of a $YBa_2Cu_3O_7$ thin film on (100) $SrTiO_3$ measured resistively and by AC susceptibility (inset).

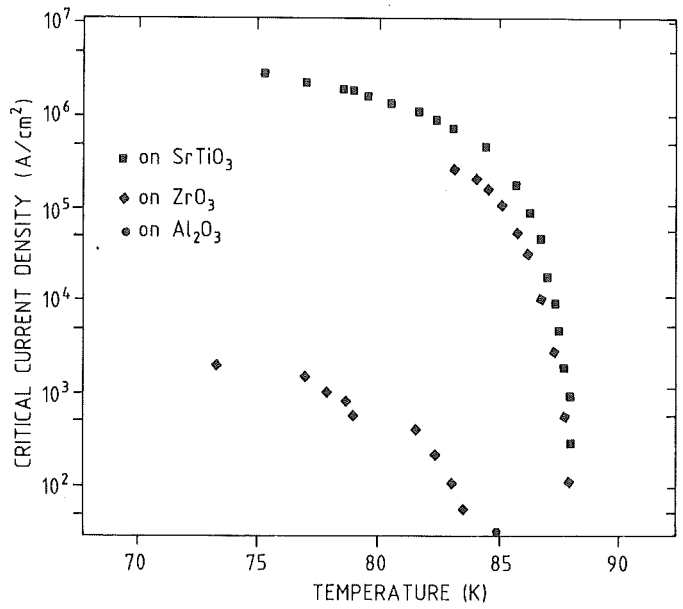

Fig. 6 Critical current density in zero magnetic field as a function of the substrate temperature for $YBa_2Cu_3O_7$ thin films deposited on various substrate materials.

could be placed in most cases several millimeters apart. Films grown on (100) $SrTiO_3$.reveal the best superconducting properties. These films show full superconductivity at 89 K with a transition width of 1.2 K. Further a sharp drop of the Al-susceptibility signal is observed at 88 K (see e.g. Fig. 5). Resistivity values at 100 K are between 70 and 150 μΩcm and resistivity ratios $\rho_{RT}/\rho_{100\,K}$ with values of about 3 were obtained routinely. Such films with thicknesses of 0.3 μm were patterned by ion beam irradiation using 600 keV Ar ions and a fluence of 1 x 10^{15} Ar^+/cm^2 at 293 K and by masking and etching with bridge sizes of 0.8 mm x 0.03 mm and 0.8 mm x 0.3 mm, respectively. The superconducting transition temperature, the width of the transition, and the critical current in zero magnetic field, I_c, were determined by the resistive method using Al strips connected with silver paste to the films. The results of such measurements are

presented in Fig. 6 where the critical current is shown as a function of temperature for films on (100) $SrTiO_3$, ZrO_2 and on Al_2O_3. The low critical current density observed for $YBa_2Cu_3O_7$ thin films on Al_2O_3 can be attributed to Josephson intergrain coupling ($I_c \approx (1-T/T_c)^{1.5}$. The highest values for the critical transport current measured up to now at 77 K in zero magnetic field were 5.4 x 10^6 A/cm^2 for $YBa_2Cu_3O_7$ films on (100)-$SrTiO_3$ 5 x 10^5 A/cm^2 for films on (100) ZrO_2 and 1 x 10^6 A/cm^2 for films on (100) MgO [34]

2. Effects of Ion Irradiation

The slowing down processes of ions in matter are well understood and a reasonable agreement exists between the measured and calculated values for the ion ranges, R_p and range distributions ΔR_p, as well as for the damage distributions. Values for R_p and ΔR_p as well as for the energy density S_n deposited in nuclear collisions may be found in tables [e.g. 53,54] or can be calculated using computer programs [e.g. 55] . The slowing down process is described in terms of two uncorrelated processes [56] (i) the inelastic interactions of the incident ions with electrons and (ii) the elastic collisions between the incident ions and the target nuclei . In the latter process large energies may be transferred to the host atoms and defects are produced by displacing host atoms from their lattice sites which in turn are able to displace further lattice atoms in

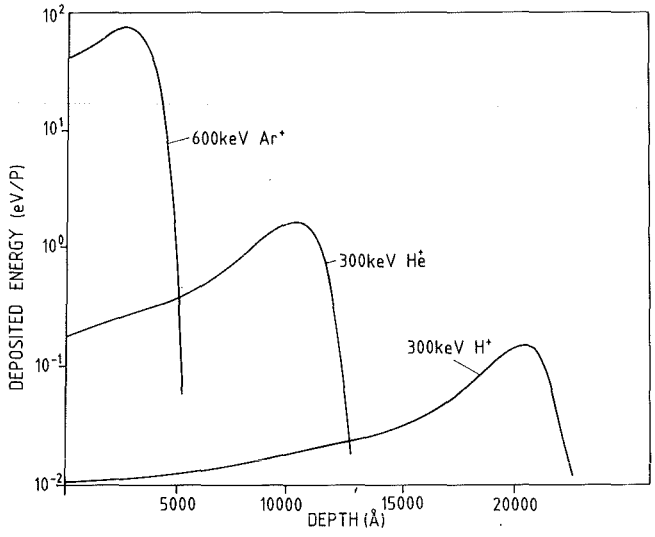

Fig. 7 Calculated deposited energy per particle for Ar-, He- and H-ions as a function of depth in $YBa_2Cu_3O_7$ using the TRIM code [55].

an avalanche-like process [57] as long as the transferred energy is greater than a minimum amount of energy, called the threshhold displacement energy, E_d.

Most frequently the linear cascade model is used in the calculations where the cascade development is considered as a chain of independent two-body collisions. Recent molecular-dynamic computer simulations [58] however indicate interactions between recoils and collective excitations which supports the longstanding ideas of the existence of a thermal spike in high density cascades [59]. These basic processes in the cascade are important to estimate the amount of damage which survives the spontaneous relaxation processes and the possible formation of damage structures. Especially in a compound system having a complicated crystalline structure special defect structures or even new phases may emerge by ultra rapid melting and cooling processes in the thermal spike region. In the following most of the irradiations have been performed with 300 keV H- and He-ions and with 600 keV Ar-ions. The energy per incident ion as a function of depth has been calculated using the TRIM program [55]. For illustration the results of such calculations are shown in Fig. 7. It is seen that He- and H-ions penetrate well the film thicknesses of about 0.3 µm generally used for the irradiation experiments. For Ar-irradiations films with thicknesses of about 0.2 µm are used. Deposited energy densities have been averaged over the film thickness. This is justified as the damage profiles especially for protons are rather homogeneous. Assuming a threshold displacement energy, E_d of 20 eV, for all the atoms of the target the number of displacements per atom (dpa) is given by $(0.8 \times S_n) / (2 \times E_d)$ [60]. The ratios of the energy densities deposited in electronic excitation to those deposited in nuclear collisions are quite different for these particles and energies and are about 1, 1×10^3 and 2×10^4 for Ar, He and H in $YBa_2Cu_3O_7$, respectively. From the fact that the T_c-decrease observed after irradiation with various ions scaled with the deposited energy into nuclear collisions it was concluded that mainly displaced atoms and not electronic excitations are responsible for the observed changes of the superconducting transition temperature [17-19] .

2.1 Transition Temperature and Conductivity

In the previous chapter it was pointed out that the superconducting properties and the resistance of the $YBa_2Cu_3O_7$ thin films strongly depend on the composition and on the growth conditions. Thin films on Al_2O_3 generally are less textured and reveal higher resistivities and lower critical currents than highly epitaxial films grown on (100) $SrTiO_3$. It is conceivable, that the rate of the T_c depression and resistance increase upon irradiation would depend on the initial properties of the starting material. This has been observed for A15 compounds,

for example for Nb_3Al and Nb_3Pt where the rate of Tc depression decreases as a function of deviation from stoichiometry [61]. In order to test this assumption films with different initial values of T_c, δT_c and ρ are used for the irradiation experiment.

The effect of H-ion irradiation on T_c and the transition width, δT_c, is shown in Fig. 8 for four thin films. Three films revealing rather large values of ρ and small values of r are deposited on Al_2O_3, while the high quality film was deposited on (100) $SrTiO_3$. The irradiations were performed at 77 K, however the data were taken after annealing to RT which causes considerable annealing of both T_c and ρ as will be discussed below. The initial unirradiated T_c-and δT_c-values of these films differ slightly. With increasing Ar-ion fluence T_c decreases and δT_c increases. The rate of suppression with fluence ($dTc/d\phi$) and the increase of δT_c clearly depend on the quality of the films. The increase of both parameters is larger for films with large values of ρ(100 K) and small values of r.

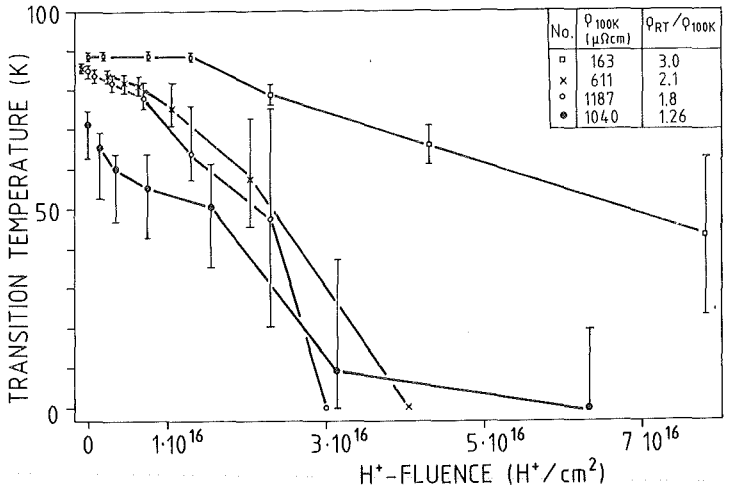

Fig. 8 Superconducting transition temperature and transition width as a function of the H ion fluence for various $YBa_2Cu_3O_7$ films of different quality.

Thus the suppression of T_c below 4.2 K is reached at smaller fluences for films of low quality. The rate of suppression for the high quality film is small at low and medium H-fluences and increases suddenly in the high fluence region. This dependence of the T_c depression rate on the film quality has been observed previously for $YBa_2Cu_3O_7$ thin films irradiated with Ar ions [27] .The large increase of δT_c with fluence as observed for the polycrystalline films, especially the fact that the T_c-onset values are less depressed than the midpoint and the downset values, may be attributed to the destruction of weak links causing the

intergrain coupling. Similar arguments have been used to explain the results obtained for neutron-irradiated sintered bulk samples [29] and ion irradiated thin films [21]. The enhanced formation of defects, especially of amorphous zones on the grain boundaries has been observed after room temperature irradiation of thin polycrystalline films with oxygen ions [20] . It may be speculated that radiation enhanced outdiffusion of oxygen near grain boundaries may support this intergrain effect. The elimination of superconductivity at higher fluences of course is clearly a bulk effect. The irradiation results obtained for the single-crystalline film are also attributed to a bulk effect especially to the radiation induced transition from the metallic into the superconducting phase as will be discussed below. The increase of the T_c depression rate for films with decreasing quality is in contrast to results observed for A15 materials mentioned above. For the A15 phases Nb-Al and Nb-Pt with various compositions it was possible to construct a master curve between T_c and Φ suggesting that the defects which are associated with the T_c depression for irradiated and for off-stoichiometric A15 structures are of similar type (anti-site defects).

It is generally agreed that the radiation sensitivity of high T_c oxides is rather high, however a quantitative comparison with that of other superconductors was hampered due to the uncertainties in the separation of bulk effects and intergrain effects of the T_c depression. In Fig. 9 we compare our results for the irradiation induced T_c depressions observed for high quality single-crystalline films of $YBa_2Cu_3O_7$ and $La_{1.8}Sr_{0.2}Cu_1O_4$ [62] with similar results obtained for other classes of superconducting materials. The normalized T_c values are shown as a function of the deposited energy in dpa for $PbMo_6S_8$ [63] , Nb_3Ge [64], V_3Si [65], NbC [66] and NbN [67]. It is seen that the radiation sensitivity of the oxide phases is higher than that of the A15 materials, however slightly lower than that of the Chevrel phases. Further it should be noted that the slope of the T_c-depression curve, especially for $YBa_2Cu_3O_7$ is rather steep which may indicate that the rapid destruction of the superconducting properties ultimately is due to a phase transition and not due to an accumulation of point defects.

The radiation induced increase of the resistivity also depends strongly on the initial resistivity values of the films. This is demonstrated in Fig. 10 where the increase of the resistivity at 100 K ($\Delta\rho = \rho(100\ K, \Phi) - \rho(100\ K, 0)$ as a function of the proton fluence is shown. For the film with the highest initial resistivity, a jump like increase of $\Delta\rho$ is seen at low fluences which may be due to the destruction of weak links between grain boundaries. For high quality films $\Delta\rho$ is

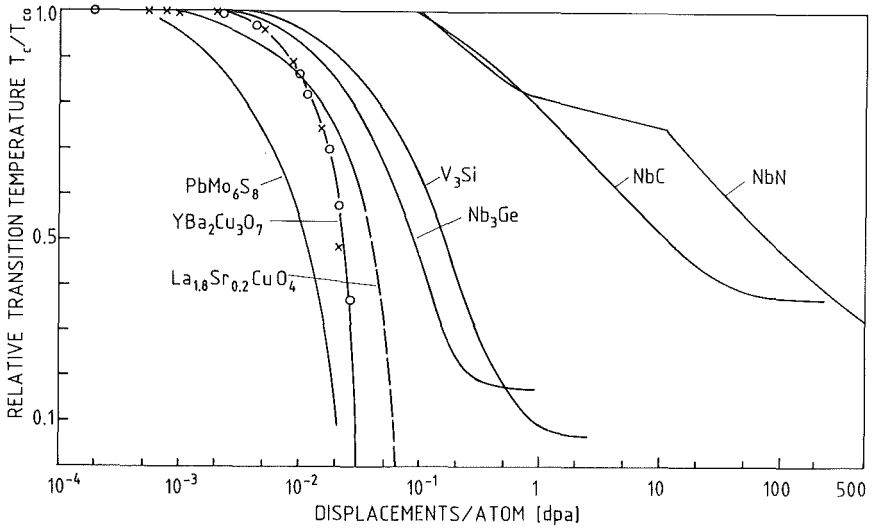

Fig. 9 Relative decrease of T_c by ion irradiation as a function of the deposited energy density in displacements per atom (dpa) for various superconducting materials.

comparatively small although for all films the resistivity increase with fluence is stronger than linear and does not saturate as is usually observed for other superconducting materials under irradiation. For these materials the increase of the resistance is proportional to ϕ and thus to the number of defect centers at low fluences and reaches a saturation at large fluences. It is interesting to correlate the T_c-decrease with the resistance increase and to compare this result with that of other superconductors [22]. Previously, the electron-phonon coupling constant λ was assumed to be proportional to $N(E_F)$ and T_c was calculated as a function of $\Delta\rho$. In Fig. 11 the relative T_c decrease, T_c/T_{co}, is presented as a function of $\Delta\rho$ in comparison to other superconductors. The results obtained for single-crystalline $YBa_2Cu_3O_7$ thin films reveal a rather small slope $d(T_c/T_{co})/d(\Delta\rho)$ of 0.01 to 0.2 $K/\Delta\Omega cm$ as compared to that of other superconductors. As can be seen in Fig. 11 remarkable differences exist in the T_c vs. $\Delta\rho$ dependence even for high quality single crystalline films. The results seem to indicate the existence of quite different threshold fluences for the T_c depression. Additional results obtained up to now show that the T_c dependence on $\Delta\rho$ depends on the incident beam direction with respect to the film orientation [68]. More experiments have to be performed in order to clarify this situation. For neutron irradiated $YBa_2Cu_3O_7$- bulk samples a nearly linear T_c vs. $\Delta\rho$ correlation was observed with no indication of a threshold fluences [30] . As the slope of $dT_c/d(\Delta\rho)$ depends strongly on the material quality, no conclusion

could be drawn on the existence of a universal correlation between T_c and the residual resistivity.

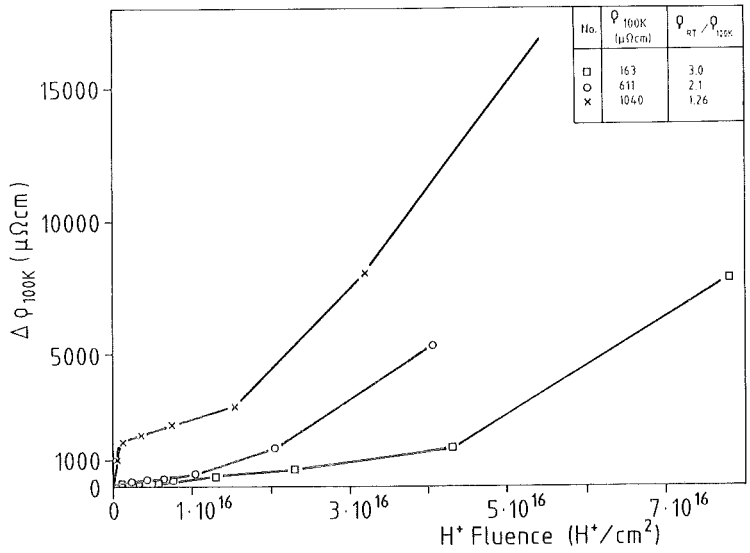

Fig. 10 Irradiation induced increase of the resistivity at 100 K as a function of the H-ion fluence for various $YBa_2Cu_3O_7$ films of different quality.

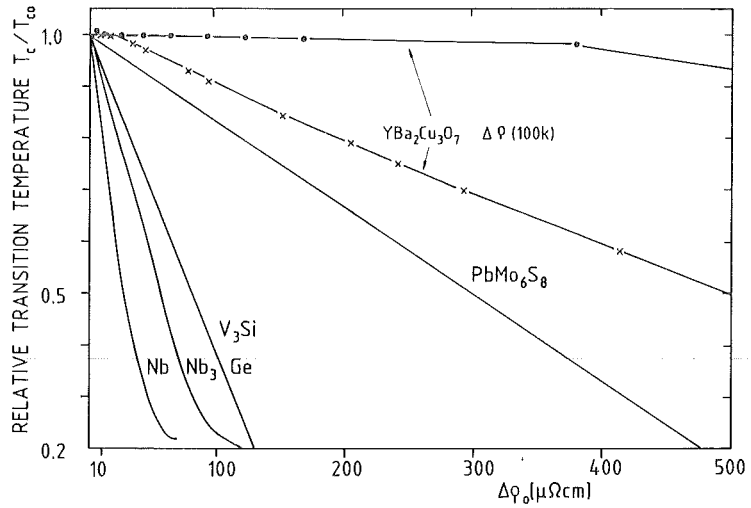

Fig. 11 Relative T_c-values as a function of the radiation induced increase of the residual resistivity for various superconducting materials.

2.2 Metal-Semiconductor Transition

In the previous chapter it was suggested that the radiation induced metal to semiconductor transition would influence the T_c depression. Detailed results on this phase transition will be presented in this and the next chapter. Before doing so we have to discuss the problem of defect mobility at and below room temperature as recovery of point defects may influence the transition process. It

is known that large recovery effects, both for T_c and $\Delta\rho$ occur after irradiation at low temperature (5K, 77 K) during annealing to 293 K [22] . This recovery has also been observed for electron irradiated bulk samples even for temperatures as low as 100 K [15] and for O ion irradiation at 293 K [24]. In situ ion irradiation of thin $YBa_2Cu_3O_7$ films at low temperatures causes a number of effects which can clearly be recognized from the results presented in Fig. 12. , where the resistance of a film is shown as a function of temperature before and after irradiation with 600 keV Ar-ions at 77 K. With increasing Ar-fluence the following main features can be observed: (i) The transition temperature to superconductivity decreases and the width of the transition increases . (ii) The resistance increases and at low ion fluences the slope dR/dT stays nearly constant. A slight increase of the slope has been observed previously after irradiation with protons at 77 K [22]. At higher fluences a semiconducting phase appears, mixed with the superconducting phase. This is obvious from the negative slope dR/dT at temperatures above 70 K for curve (c). (iii) A strong annealing stage can be noted at temperatures above 150 K. This feature can be evaluated from the annealing curve (c) in comparison with the heating and cooling curve (d). Curve (c) was obtained after irradiation with a total dose of 6 x 10^{13} Ar-ions/cm^2 at 77 K then cooled to 6 K and annealed to 296 K. The sample was then remeasured and curve (d) was obtained. In comparing curves (c) and (d) it is seen that about 60% of the irradiation induced resistance increase at 100 K recovered upon warming up to 296 K. From our previous results [22] we can state that after irradiation at 6 K the heating and cooling curves between 5 and 120 K are the same and we concluded that there is no strong defect recovery stage below about 120 K.

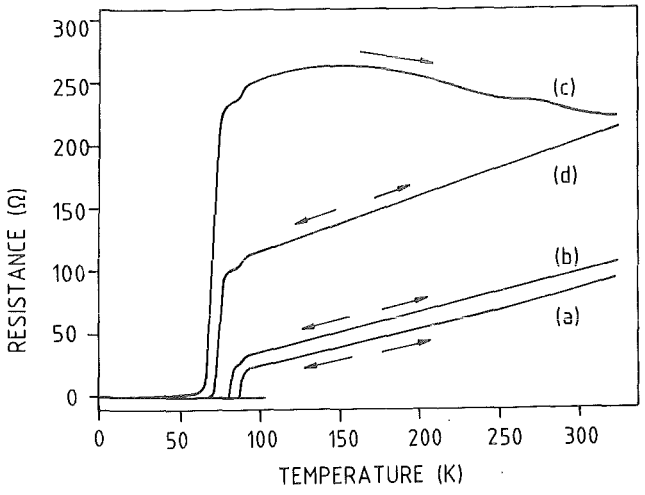

Fig. 12 Resistance vs. temperature: heating and cooling curves of a sample before (a) and after irradiation with a total fluence of 6 x 10^{12} Ar^+/cm^2 at 6 K and annealed to 325K (b). Heating curve of the same sample after irradiation with 3 x $10^{13}Ar^+/cm^2$ at 6 K (c) and cooling and heating curve after annealing to 325 K(d).

In order to avoid the influence of recovery on the damage production rate, irradiations with protons have been performed at 77 K and the resistance increase was determined at 100 K without any further annealing to higher temperatures. The results of this measurement are shown in Fig. 13, where $\Delta\rho$ is plotted as a function of the deposited energy density in dpa. For comparison the behaviour of the transition temperature for two irradiated single crystalline films is shown on the same dpa scale. Three different dpa regions of the $\Delta\rho$ increase can be recognized (this is more clearly seen from the slope $d(\Delta\rho/d\phi)$ and we will tentatively call the first region the metallic one (for dpa-values up to 1.5×10^{-2} dpa) followed by the transition region from the metallic to the semiconducting phase which is completed at about 4×10^{-2} dpa, followed by a transition into the amorphous phase which is not yet completed at about 0.13 dpa. More arguments for this arrangement will be presented in the next chapter on defect structures. It can be seen that T_c starts to decrease already in

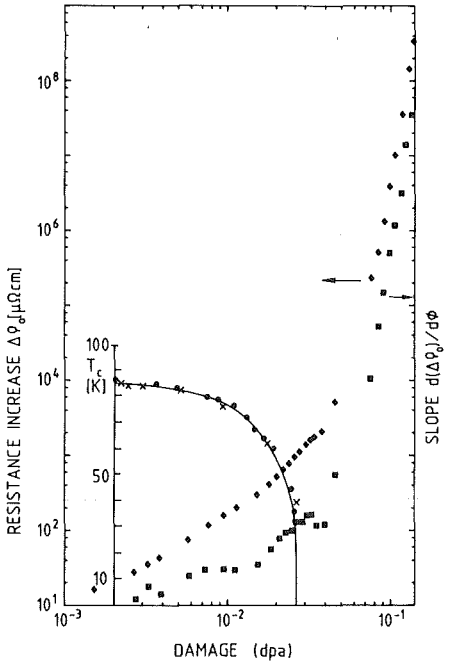

Fig. 13. Resistance change at 100 K and transition temperature as a function of the deposited energy density in dpa.

the metallic region due to point defect production. The elimination of the superconductivity occurs in the transition region where metallic and semiconducting phases coexist and is probably finished with the completion of the phase transition [22,27] . The mixture of a superconducting (metallic) phase and semiconducting phases is clearly demonstrated by the resistance vs. temperature curve shown in Fig. 14a. This sample was irradiated with 1.1×10^{17} H+/cm^2 at 5 K ($\approx$0.02 dpa). After annealing to 325 K a fraction of the material recovered and

became again superconducting. It can be seen in Fig. 14a that now the cooling and heating curve consists of at least two phases. The steep increase of the resistance with decreasing temperature in the region below 10 K and also above 70 K indicate an activated conduction. The question arises if hopping conduction prevails $\sigma \approx \exp(-A/T^{1/4})$ or excitation to a gap energy $\sigma \approx \exp(E_g/kT)$. The data of Fig. 14a are replotted in Fig. 14b where the natural logarithm of the resistance, ℓnR, is given as a function of 1/T. In this plot two linear regions are noted: the linear region above about 100 K which can be fitted using a gap value of about 10 meV, while for the region between 5 K and

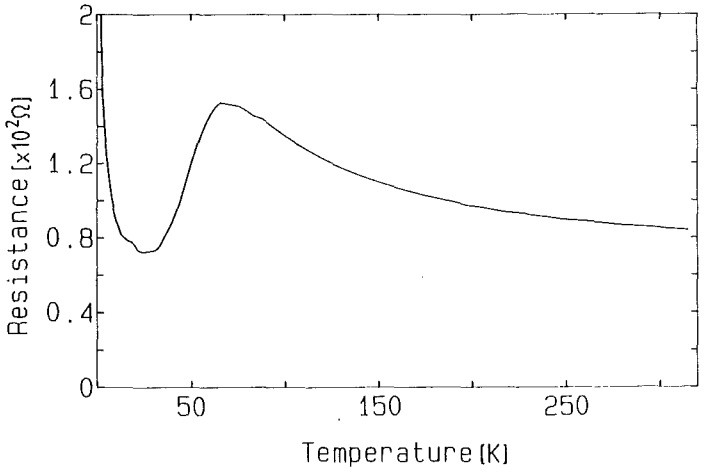

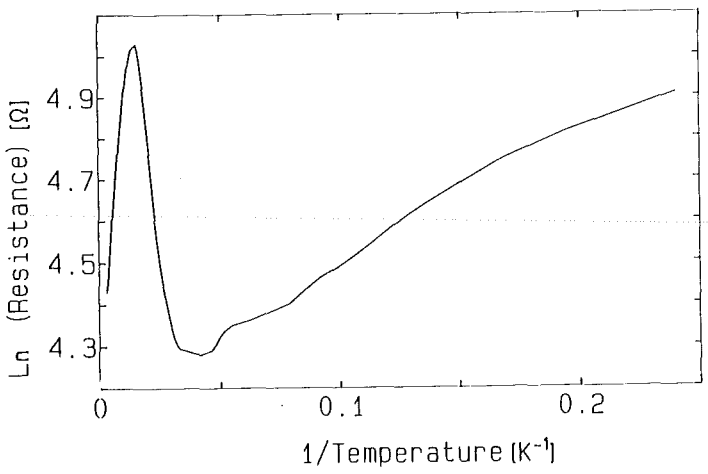

Fig. 14 (a) Resistance vs. temperature after irradiating the sample with a total dose of 1.1 x 10^{17} H+/cm², 300 keV at 77 K and annealing to 293 K. (b) Resistance vs. the inverse temperature of the same sample.

10 K. gap energy E_g of 0.36 meV can be obtained. Here we tentatively assume that a semiconducting phase forms and from the activation energies immediately the gap energies can be deduced. This may be questioned and is discussed in more detail below. For the low temperature region deviations from the straight line are noted at temperatures below 5.5 K, which indicates that additional processes contribute to the thermally activated conduction. Thus the

temperature dependence of the resistivity curves shown in Fig. 14a and b seem to indicate the coexistence of three phases: (a) the metallic (superconducting) phase, (b) a phase having a rather small activation energy and (c) a semiconducting phase. The latter phase dominates with increasing fluence. The energy gap values change by annealing as well as by irradiation. Before annealing to 325 K the sample shown in Fig. 14a reveals a gap value of 0.9 meV in the low temperature region. The gap value in the high temperature region which prevails at larger fluences increases with increasing deposited energy density as is shown in Fig. 15. From the results obtained up to now an energy gap is observed which increases with a slope of about 1.5 eV/dpa. No saturation is seen as the completely amorphous state is not yet reached. Large gap values of 0.2 and 0.42 eV have been published recently for deposited energy densities 0.26 and 0.37 dpa, respectively [24]. These gap values are smaller than those calculated using the slope given above which indicates that a saturation is approached.

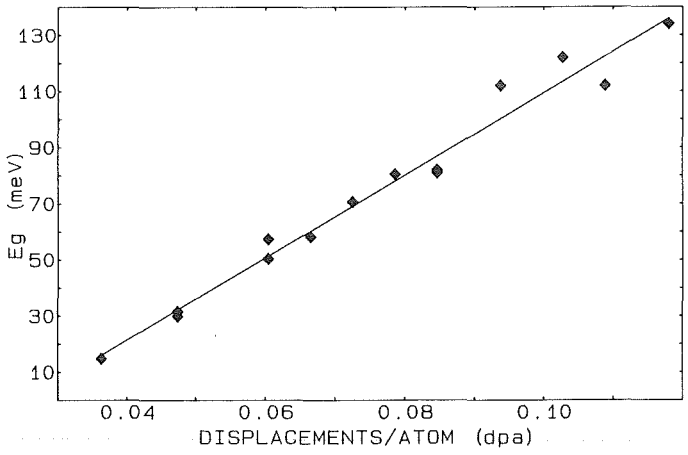

Fig. 15 Energy gap as a function of the deposited energy density in dpa.

Several processes may contribute to the ion induced metal-insulator transition. It is well known that by reducing the oxygen content, N from 7 to 6.5 an . orthorhombic to tetragonal phase transition occurs where the resistivity of the compound changes from metallic to semiconducting. The activation energy for the semiconducting phase changes from $\approx$0.07 eV to 0.37 eV for N from 6.5 to 6.25 [69]. The band gaps E_g deduced from the activation energies would range between 0.14 and 0.72 eV, the latter value is far larger than that obtained by high dose ion irradiation. Nevertheless, it is suggested that the radiation induced phases are due to oxygen displaced from their lattice sites. Oxygen loss by outdiffusion during irradiation at 293 K and below can be excluded by experiment [70] . Previously it was suggested that knocked out O-atoms would

not go into stable interstitial positions because there are many O-vacancies between the chains which would act as deep traps [15]. Indications for a random occupation of lattice sites in the Cu(1) plane has been observed by X-ray diffraction [27] and will be discussed below.

Another possible mechanism causing the metal to semiconductor transition is the shift of the Fermi energy in regions with negligible density of electronic states . This may be caused by an increase of the unit cell as observed by X-ray diffraction [24,27]. The metal to semiconductor transition at N = 6.5 as observed by varying the oxygen content has been interpreted as supporting the Hubbard model for the bandstructure near the Fermi level [69].

For the ion induced semiconducting phases the experimental situation is not yet settled. The observed dependences of ℓnR on T vary from T^{-1}, to $T^{-1/2}$ [71a] to $T^{-1/4}$ [71b]. The latter dependence was obtained for low fluences and temperatures . A $T^{-1/4}$ dependence would be in accordance with charge carrier localization [72] where the conduction at low temperatures is due to variable range hopping. Our data at low doses and low temperatures are better described by a 1/T dependence of ℓnR, although deviations from this dependence occur at temperatures below 5 K. Hall effect and/or thermoelectric power measurements are necessary to study the dependence of the carrier density and the mobility on the fluence and on the temperature in order to decide if the thermally activated conduction is by exciting electrons across a gap into the conducting band or correspondingly creating holes in the valence band or is due to a strong temperature dependence of the carrier mobility reflecting a diffusion process through a potential energy barrier. First Hall measurements on irradiated samples [69a,b] indicate only a slight dependence of the Hall number on the ion fluence as well as on the temperature which could not account for the large changes observed for $\rho(\phi)$ and for $\rho(T)$.These preliminary results suggest that the mobility and its temperature dependence probably affect the conduction process to a larger extent.

2.3 Defect Structures

Radiation induced defect structures in $YBa_2Cu_3O_7$ have been studied by TEM [20,73,74] by X-ray diffraction [19,27,75] and by ion channeling [21,50]. Extended defect formation is observed after prolonged electron irradiation of

the single crystalline orthorhombic phase below 50°C [73] . Threshold energies determined for oxygen atom displacement were near 20 eV. The observed motion of twin boundaries and the shrinkage of the twinned volume implies a movement of oxygen in the basal plane. Irradiation of $YBa_2Cu_3O_y$ ($5.8 < y < 6.5$) with 1 MeV electrons in a high electron energy transmission electron microscopy indicated the disordering of the BaO- and Y-layers, forming a cubic superlattice structure [74]. No extended defects ,e.g., dislocation loops were observed by TEM studies of oxygen irradiated polycrystalline thin films [20,75] . Low doses of oxygen ions produced thin amorphous layers on the grain boundaries.

The crystalline to amorphous transition was also studied with X-ray diffraction. The intensity of the (006) reflex decreased suddenly after a critical dose of oxygen ions of about 0.1 dpa, which is low compared to other oxides with perovskite structure [75] . The decrease of X-ray line intensities is demonstrated in Fig. 16, where some spectra are shown before (a) and after irradiation of polycrystalline $YBa_2Cu_3O_7$ thin films with 300 keV He ions at 77 K at fluences of 8 x 10^{16}(b), 1.5x10^{17}(c) and 3.6 x 10^{17} H^+/cm^2(d).

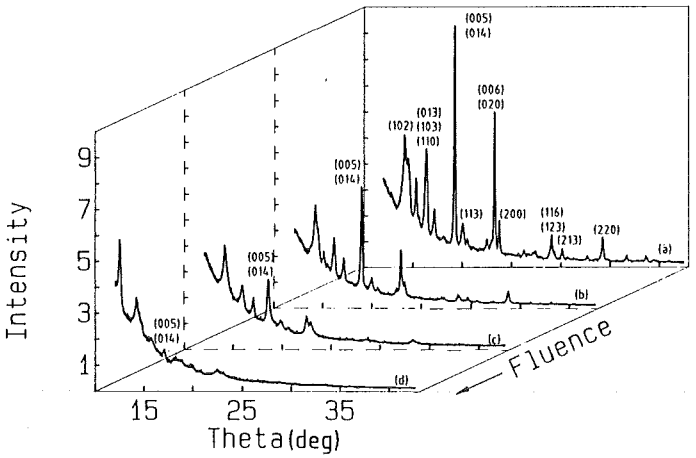

Fig. 16 Relative X-ray intensities as a function of the scattering angle Θ. (a) for the as-grown $YBa_2Cu_3O_7$ film and (b,c,d) after irradiation with 8x10^{16},1.5x10^{17} and3.6x10^{17} H^+/cm^2.

After irradiation the films were warmed up to room temperature and transferred to a Seemann-Bohlin thin film diffractometer. Fig. 16 shows that the line intensities decrease strongly with increasing proton fluence which indicates that a certain fraction of atoms is displaced from their lattice sites and do no longer contribute to the coherent scattering. Complete amorphization is not yet obtained although the total deposited energy was about 0.1 dpa. This may be due to the light ion mass used, where the average transferred energy and therefore the average cascade density is smaller than for the oxygen ion irradiations mentioned above. The line intensity weakening in irradiated samples, especially at high diffraction angles suggested the use of the

temperature factor concept applying the modified Wilson plot. This technique was previously successfully used to determine local atomic displacements around vacancies in refractory materials [76] as well as static displacements and amorphous fractions in V_3Si [77] . First attempts [27] to obtain the amorphous fraction in irradiated $YBa_2Cu_3O_7$ thin films using modified Wilson plots reveal a rather good agreement with the results obtained by ion channeling [27] although the accuracy was limited. The intensity ratio of a group of X-ray lines I(006,(020))/I(200) which is about 0.63 in the tetragonal phase and 4.4 in the orthorhombic phase was studied as a function of the fluence after proton irradiation at 77 K and annealing to 296 K. The intensity ratio of the non-separated (020) and (006) lines to the (200) line decrease from 4.4 to 1.4 (Fig. 16).

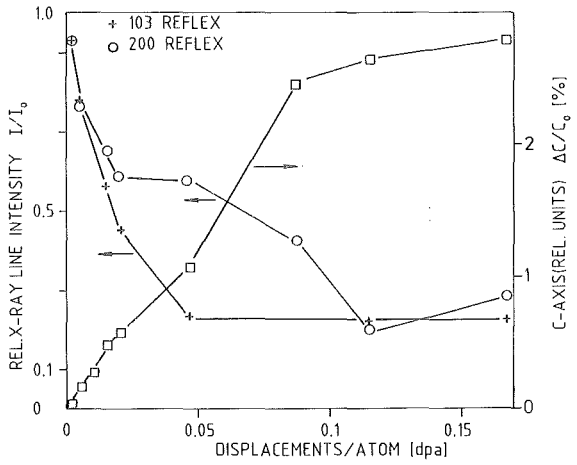

Fig. 17 Relative X-ray intensities for the (103) and (200) reflex and relative change of the c-axis as a function of the deposited energy density in dpa.

This indicates that there is a tendency for a random occupation of oxygen vacancies with oxygen atoms during irradiation, equivalent to an orthorhombic to tetragonal phase transformation during irradiation [27] . The intensity decrease with increasing fluence varies strongly for different reflexes. In Fig. 17 the relative intensities for the (103) and (200) reflexes are shown as a function of the deposited energy density in dpa. Although a strong decrease of the line intensities is noted at small dpa-values, the lines do not disappear completely indicating that some polycrystalline material is still present even at 0.15 dpa. Further it is shown in Fig. 17 that the lattice continuously expands under irradiation. A saturation value of about 2.8% for the expansion is reached with increasing fluence. This value is in good agreement with results obtained after O and As ion irradiation [75,24] .

Defect structures in the past have been determined by X-ray diffraction and by ion-channeling. For the analysis of defects in A15 superconductors these techniques yielded complementary results in different defect density regions [77]. Channeling analysis of irradiated single crystalline $YBa_2Cu_3O_7$ thin films at 2 MeV has been applied to determine the fraction of displaced atoms in the metal sublattice. It was clearly shown that the same number of atoms in the Ba, Y and Cu sublattice were displaced during the irradiation with 2 MeV He ions at room temperature [50] . In Fig. 18 the random and <100> aligned backscattering and channeling spectra before and after irradiation with 2.6 x 10^{16} He^+/cm^2 at 3.04 MeV are shown. As discussed in the first chapter He ion channeling together with the resonance scattering of He on oxygen at 3.04 MeV was used to determine the oxygen content and to study the damage production and annealing in the oxygen sublattice. From the increase of the peak area of the oxygen peak and from the increase of χ_{min} in the Ba, Y and Cu-region it is concluded that about 13% of the metal atoms and about 16% of the oxygen atoms have been displaced by depositing an energy density of about 0.01 dpa. Irradiation with 3.4x10^{16} He^+/cm^2, 1 MeV at 77 K (0.04 dpa) leads to an increase of 30% for the displaced atom fraction in the metal sublattices and of about 50% in the oxygen sublattice. Considering the higher sensitivity for the scattering of He-ions on slightly displaced O-atoms (due to the flux distribution in the channel) it is concluded that nearly the same amount of atoms is displaced in each sublattice after irradiation at 296 K. However, if we assume that oxygen atoms are randomly displaced, then the metal atoms should have an average threshold energy for displacement slightly above that of oxygen. Warming up to 293 K and remeasuring at 77 K did not reveal any recovery effect. This is in contrast to the large recovery stage of the resistance observed below 296 K. Therefore it is assumed that the recovery of the radiation enhanced resistance is due to the recombination of O-atoms which had been displaced to positions not visible by channeling analysis along the c-axis. Therefore the visible displaced oxygen atoms would belong to disordered regions which will not anneal by warming up to 293 K, while the annealing stage at 293 K and below is due to oxygen displaced to oxygen vacancies (not visible by channeling) and performing some ordering jumps upon annealing in order to achieve local charge neutrality.

Most of the irradiation experiments have been conducted using the superconducting othorhombic phase. The question arose if the intrinsic damage introduced during thin film growth as well as the radiation induced damage is different in the tetragonal phase. First channeling results indicate that the

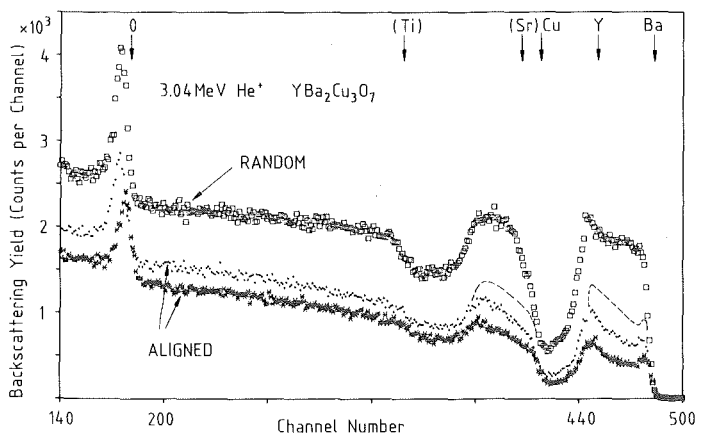

Fig. 18 Random and <100> aligned backscattering spectra from an $YBa_2Cu_3O_7$ thin film. The aligned spectra are shown after irradiation with 1 MeV He ions.

standard deviation of the crystallite orientation distribution from the (100) $SrTiO_3$ direction also for the tetragonal phase is 0.2°, similar as that observed for the orthorhombic phase. The main defects incorporated during film growth are low angle dislocations [23]. Concerning the radiation induced defect structure as determined by ion channeling, no difference is noted concerning the defect production rate. The angular yield curves for the Ba-sublattice of the tetragonal phase are shown in Fig. 19.

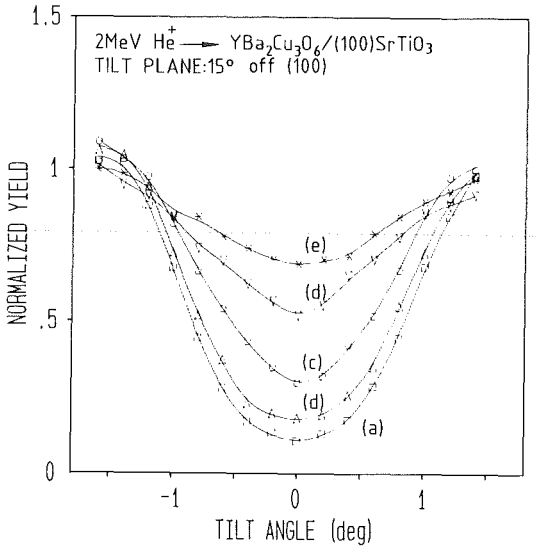

Fig. 19 Angular scan curves through the <100> axial direction of an $YBa_2Cu_3O_6$ thin film.
The yield for Ba is shown after irradiation with various fluences of 2 MeV He ions ($1.5x10^{16}$(b), $3.4x10^{16}$(c), $5.2x10^{16}$(d) and $7.5x10^{16}$ He^+/cm^2.

It can be seen that the minimum yield increases continuously with 2 MeV He ion irradiation at room temperature. Further it is noted that the critical angles decrease indicating an increase of a static Debye Waller factor. In order to determine if the increase of the minimum yield, X_{min} is due to the fraction of displaced atoms and not due to the production of extended defects, energy

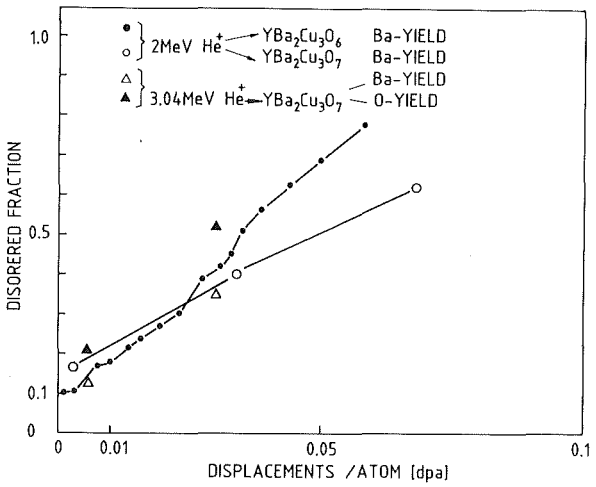

Fig. 20 Disordered fraction of Ba and O atoms as a function of the deposited energy density in dpa after irradiation with 2 and 3.05 MeV He-ions.

dependent measurements have to be performed which are in progress [78]. The increase of the disordered fraction which is equal to X_{min} is plotted as a function of the deposited ion energy in dpa (Fig. 20). Included in this figure are some results for the orthorhombic phase (open circles) and for oxygen. At about 0.1 dpa (extrapolated) amorphization would occur in good agreement with X-ray diffraction data. It should be noted that at about 0.03 dpa where the superconductivity is eliminated, already about 30 to 40 vol.% of the material is disordered corresponding to about 2.3×10^{21} displaced atoms/cm^3. However, the dpa-.value of 0.03 corresponds to about 2.3×10^{22} displacements/cm^3 which is about a factor of 10 smaller than the value obtained from X_{min}. Currently the source of this discrepancy is not clear. One hypotheses could be the formation of disordered region by rapid quenching from non-linear cascade regions [58] . Further studies are obviously required to solve this question. In general, it is remarkable that the damage structures observedfor $YBa_2Cu_3O_7$, such as point defects, amorphous zones and static displacements where all host atoms are displaced from their lattice sites by about 0.07 Å , resemble very closely similar damage structures observed for other cluster compounds. This provides an explanation for the fact that the superconducting properties of these compounds reveal similar sensitivity to radiation induced disorder.

3. Applications

Ion implantation is a versatile non-equilibrium technique to modify the physical properties of materials. The changes of the material properties are due to chemical or alloying effects caused by the implanted ion species and due to disorder, produced by the interaction of the ions with the host atoms during the slowing down process. The influence of both effects on the property changes have to be separated. In the previous chapter mainly the influence of disorder has been discussed as the incident ions penetrated the thin films and came to rest in the substrate. In the application of ion beams for materials modification both processes, implantation and irradiation have to be considered. The results obtained by ion implantation into conventional superconductors have been reviewed [79,80]. Ion implantation has been used to produce new and metastable alloys, e.g. supersaturated solid solutions and to improve compounds by compensating deviations in composition from stoichiometry. Three main areas for the application of ion implantation have been explored: (i) increasing the pinning forces to enhance the surface current carrying capacity (ii) reduction of rf losses at superconducting surfaces and (iii) production of weak links. The results are summarized in ref. [79] . With the availability of single crystalline thin oxide films the use of ion beams has been explored for the modification of the high T_c superconductors.

First implantation experiments have been reported for the fabrication of $La_{1.8}Sr_{0.2}CuO_4$ films (nominal composition) and of $YBa_2Cu_3O_7$ thin films [25]. $YBa_2Cu_3O_7$ thin films have also been synthesized by ion beam mixing [81,81a]. After implanting Sr ions in La/Cu multilayer films and annealing in flowing oxygen at 500°C the films became superconducting revealing a broad transition. The transition curves were very sensitive to the annealing conditions. The superconducting layer was buried beneath the surface [25] . Since the oxygen incorporation from the environment may be limited by surface barrier diffusion oxygen was implanted in amorphous $La_{1.8}Sr_{0.2}CuO_4$ layers at 77 K and a two step annealing in air was applied. An improvement of the T_c onset value was observed in contrast to similarly treated non-implanted thin films [34] . By ion implantation $YBa_2Cu_3O_7$ becomes amorphous and an important question is if solid state epitaxy would occur starting preferentially at the interface between amorphous film and oriented substrate surface. First attempts to test this were not successful. Although some regrowth did occur, channeling and

backscattering indicated that the substrate layer was not a preferred nucleation site for monolayer by monolayer growth [25] . Ion beam mixing is a well known technique to intermix atomic species at the interface of thin film couples within the collision cascade and simultaneously avoid the material loss due to sputtering at the bombarded surface [82]. This techique has been used to intermix $BaO/Y_2O_3/Cu$ layered structures by bombarding these couples with Xe- or O-ions (200-300 keV) at temperatures below 500°C. After annealing the mixed films in O_2 at temperatures below 600°C, the films were orthorhombic and superconducting [81] .

Particle implantations and irradiation of superconductors often leads to an enhancement of the critical current capacity due to the production of damage structures which act as pinning centers. By neutron irradiation of $YBa_2Cu_3O_{7-x}$ bulk single crystals the critical magnetization current has been enhanced [28,84] This rises the question how critical transport currents in single crystalline $YBa_2Cu_3O_7$ thin films are affected by intrinsic defects and by defects produced during irradiation. In order to study the influence of radiation induced defects on I_c, narrow bridges of the $YBa_2Cu_3O_7$ thin films on $(100)SrTiO_3$ and $(100)Zr(Y)O_2$ have been irradiated at 293 K with 300 keV protons. In Fig. 21 the

Fig. 21 Critical current as a function of the deposited energy density in dpa for $YBa_2Cu_3O_7$ thin films on $SrTiO_3$ and $ZrO(Y)_2$.

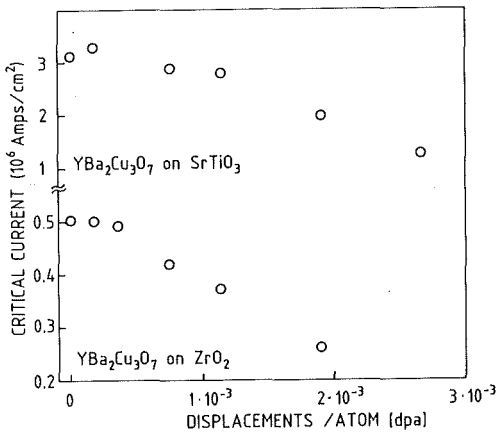

critical current at 77 K in zero field is shown as a function of the deposition energy density in dpa. It is seen that the critical current immediately decreases even in a dpa-region where only a small decrease of T_c is observed (see Fig.13 for comparison). Similar results have also been observed after irradiation of epitaxial $YBa_2Cu_3O_7$ films with 1 MeV Ne ions at 300 K [83] . The average spacing between

fluxoids is of the order of 300 Å [31]. For the lowest irradiation fluence used in Fig. 21 we have about 1.5 x 10^{19} displacements/cm3, corresponding to an average spacing of about 46 Å between displacements. Assuming the displacements to act as pinning centers, then with increasing density the fluxoids would overlap at a scale of the coherence length ($\approx$30 Å) and move easily between pinning centers. Thus the critical current would greatly be reduced. It seems that the intrinsic defect density in single-crystalline thin films is optimal for flux pinning. Besides twins, low angle dislocations may act as pinning centers.

Ion beam patterning has been used to form fine structures like narrow bridges for critical current measurements and for the production of superconducting quantum interference devices (SQUID) [84,24]. Here the radiation induced metal to insulator transition is used for patterning circuits onto thin films of $YBa_2Cu_3O_7$.. The patterning process is rather simple and has been described already in chapter 1. A more elaborate processing sequence was used for SQUID production such as an evaporation of a gold film, (b) negative organic resist spun onto the gold and photolithography (c) argon milling of the exposed gold and then finally (d) ion implantation [84]. Using the controlled reduction of the critical current by ion irradiation without affecting the transition temperature to a large extent, the sensitivity of SQUID's could be enhanced [83].

4. Conclusions

Ion beam modification and analyses has provided a wealth of information within a short period of time. The analysis of numerous thin films by ion backscattering spectrometry made it possible to optimize the various sputtering parameters in such a way that films with stoichiometric composition were grown. Film compositions and interface reactions were monitored to optimize different annealing and growth conditions. The preparation of nearly defect free single crystalline surfaces of the various substrates was analyzed and optimized using ion channeling combined with backscattering. The growth of $YBa_2Cu_3O_7$ thin films on these substrate surfaces was monitored and intrinsic damage structures were analyzed using the ion beam technique. The films optimized in this way revealed a high single crystalline quality and good superconducting properties which often exceeded those of bulk single crystals.

The high T_c oxides are sensitive to damage produced by ion irradiation. Defect structures as analyzed by ion channeling are mainly point defects, small static displacements of all lattice atoms from their lattice sites by about 0.07 Å and amorphous zones. Nuclear collisions and probably dense cascade effects are the main source for the observed property modifications. The T_c depression and the resistance increase with increasing ion fluence depends on the microcrystalline structure indicating that grain boundaries play a large role in polycrystalline films. For single crystalline films the elimination of superconductivity occurred in a fluence region where both metallic and semiconducting phases are mixed, which indicated that a phase transition is reponsible for the disappearance of the superconductivity. With further increasing the ion fluence the activation energy of the insulating phase increased and a transformation in the amorphous phase occured. This metal to insulator transition had been successfully used for ion beam patterning to fabricate narrow bridges, to measure critical currents and for the production of SQUID's.The critical current immediately decreased upon low dose irradiation which indicated that the intrinsic damage in the as-grown films provided optimal pinning of fluxoids. The sensitivity of the SQUID's was improved by lowering the critical current without affecting T_c to a large extent. Ion implantation and ion beam mixing was used to produce high T_c oxide materials. Much remains to be learned about both the electronic and the structural properties of ion irradiated and implanted oxide materials. An increase in understanding in this respect will certainly be followed by an improvement of superconducting properties.

ACKNOWLEDGEMENT

The author would like to thank his colleagues L. Abu-Hassan, B. Egner, J. Geerk, H.C. Li, Qi Li, G. Linker, F. Ratzel, J. Remmel, R. Smithey, B. Strehlau, F. Weschenfelder, G.C. Xiong and X.X. Xi for valuable discussions and for providing some of their results prior to publication.

REFERENCES

[1] Proc. of the International Discussion Meeting on Radiation Effects on Superconductors, J. Nucl. Mat. **72** (1978) 1-300

[2] L.F. Mattheiss and R.L. Testardi, Phys. Rev. B**20** (1979) 2196, Phys. Rev. Lett. **41** (1978) 1612

[3] A.R. Sweedler and D.E. Cox, Phys. Rev. B**12** (1975) 147

[4] R.D. Blaugher, R.E. Heim, J.E. Cox and R.M. Waterstrat, J. Low Temp. Phys. **1** (1969) 539

[5] R. Schneider, G. Linker and O. Meyer, Phys. Rev. B**35** (1987) 55

[6] O. Meyer, J. Nucl. Mat. **72** (1978) 182

[7] O. Meyer, R. Kaufmann, B.R. Appleton and Y.K. Chang, Solid State Comm. **39** (1981) 825

[8] A. Guha, M.P. Sarachik, F.W. Smith and L. R. Testardi, Phys. Rev. B**18** (1978) 9

[9] M. Grimsditch, K.E. Gray, R. Bhadra, R.T. Kampwirth and L.E. Rehn, Phys. Rev. B**35** (1987) 883

[10] N. Nücker, J. Fink, J.C. Fuggle, P.J. Durham, W.M. Temmermann, Phys. Rev. B**37** (1988) 5158

[11] J.M. Tarascon, W.R. McKinnon, L.H. Greene, G.W. Hull, and E.M. Vogel, Phys. Rev. B**36** (1987) 883

[12] J. van den Berg, G.J. van der Beek, P.H. Kes, G.J. Nienwenhuys, J.A. Mydosh, H.W. Zandenbergen, F.P.F. van Berkel, R. Steems and D.J.W. Ijdo, Europhys. Lett. **4** (1987) 737

[13] B.G. Bagley, L.H. Greene, J.M. Tarascon and G.W. Hull, Appl. Phys. Lett. **51** (1987) 622

[14] Y. Quere, Nucl. Instr. and Meth. B**33** (1988) 906 and references therein

[15] N. Moser, A. Hofmann, P. Schüle, R. Henes, and H. Kronmüller, Z. Phys. B 71 (1988) 37; Physica C**153-155** (1988) 341

[16] V.F. Zelenskij, I.M. Neklyndov, Yu. T. Petrusenko, A.N. Sleptsov and V.A. Finkel, Physica C**153-155** (1988) 850

[17] G.J. Clark, A.D.Marwick, R.H. Koch and R.B. Laibowitz, Appl. Phys. Lett. **51** (1987) 139

[18] J. Geerk, H.C. Li, G. Linker, O. Meyer, C. Politis, F. Ratzel, R. Smithey, B. Strehlau, X.X. Xi and G.C. Xiong, Z. Phys. B - Condensed Matter **67** (1987) 507

[19] B. Egner, J. Geerk, H.C. Li, G. Linker, O. Meyer, and B. Strehlau, Jap. J. of Appl. Phys. **26** (1987) (Suppl. 26-3) 2141

[20] G.J. Clark, F.K. LeGoues, A.D. Marwick, R.B. Laibowitz, and R. Koch, Appl. Phys. Lett. **51** (1987) 1462

[21] A.E. White, K.T. Short, D.C. Jacobson, J.M. Poate, R.C. Dynes, R.M. Mankiewich, W.J. Skocpol, R.E. Howard, M. Anzlowar, K.W. Baldwin, A.F.J. Levi, J.R. Kow, T. Hsieh, M. Hong, Phys. Rev. B (1988) 3755

[22] G.C. Xiong, H.C. Li, G. Linker, O. Meyer, Phys. Rev. B38 (1) (1988); Physica C**153-155** (1988) 1447

[23] O. Meyer, B. Egner, J. Geerk, R. Gerber, G. Linker, F. Weschenfelder, X.X. Xi, and G.C. Xiong, 7th Int. Conf. on Ion Implantation Technology, IIT'88; June 1988 Kyoto Japan, to be published in Nucl. Instr. and Meth. B; F. Weschenfelder et al. to be published.

[24] A.D. Marwick and G.J. Clark, ibid. to be published in Nucl. Instr. and Meth. B

[25] A.E. White, K.T. Short, J.P. Gamo, R.C. Dynes, L.F. Schneemeyer, J. Waszczak, A.F.J. Levi, M. Anzlowar, and K.W. Baldwin, ibid. to be published in Nucl. Instr. and Meth. B

[26] D.B. Chrisey, G.P. Summers, W.G. Maisch, E.A. Burke, W.T. Elam, H. Herman, J.P.Kirkland and R.A. Neiser, Appl. Phys. Lett. **53** (1988) 1001

[27] O. Meyer, B. Egner, G.C. Xiong, X.X. Xi, G. Linker and J. Geerk, 6th Int. Conf. on Ion Beam Modification of Materials, June 1988, Tokyo, Japan, to be published in Nucl. Instr. and Meth. B

[28] A. Umezawa, G.W. Crabtree, J.Z. Lin, H.W. Weber, W.K. Kwok, L.H. Nunez, T.J. Moran, C.H. Sowers, H. Claus, Phys. Rev. B **36** (1987) 167

[30] P. Müller, H. Gerstenberg, M. Fischer, W. Schindler, J. Stöbel, G. Saemann-Ischenko, H. Kammermeier, Solid State Commun. **65** (1988) 223, Physica C**153-155** (1988) 343

[31] P. Chaudhari, R.H. Koch, R.B. Laibowitz, T.R. McGuire, and R.J. Gambino, Phys. Rev. Lett. 58 (1987) 2684; Jap. J. Appl. Phys. **Z6** (1987) Suppl. 26-3, p. 2023

[32] T.R. Dinger, T.K. Worthington, W.j. Gallagher and R.L. Sandstrom, Phys. Rev. Lett. **58** (1987) 2687

[33] H. Adachi, K. Setsune, T. Mitsuyu, K. Hirochi, Y. Ichikawa, T. Kamada and K. Wasa, Japanese J. of Appl. Phys. **26** (1987) L709

[34] X.X. Xi, G. Linker,O. Meyer, E. Nold. B. Obst, F. Ratzel, R. Smithey, B. Strehlau, to be published in Z. f. Phys. - Condensed Matter

[35] M. Kawasaki, S. Nagota, Y. Sato, M. Funabashi, T. Hasegawa, K. Kishio, K. Kitazawa, K. Fueki and H. Koinuma, Japanese J. of Appl. Phys. **26** (1987) L738

[36] L. Li, B. Zhao, Y. Lu, H. Wang, Y. Zhao, and Y. Shi, Chinese Phys. Lett., Vol. **4**, No. 5 (1987)

[37] R.E. Somekh, M.G. Blamire, Z.H. Barber, K. Butler, J.H. James, G.W. Morris, E.J. Tomlinson, A.P. Schwarzenberger, W.M. Stobbs, and J.E. Evetts, Nature, Vol. **326** (1987) 857

[38] M. Naito, D.P.E. Smith, M.D. Kirk, B. Oh, M.R. Hahn, K. Char, D.B. Mitzi, J.Z. Sun, D.J. Webb, M.R. Beasley, O. Fischer, T.H.Geballe, R.H. Hammond, A. Kapitulnik, C.F. Quate, Phys. Rev. B**35** (1987) 7228

[39] O. Fischer, T.H. Geballe, R.H. Hammond, A. Kapitulnik, and C.F. Quate, Phys. Rev. B**35** (1987) 7228

[40] J. Kwo, T.C. Hsieh, R.M. Fleming, M. Hong, S.H. Liou, B.A. Davidson, and L.C. Feldman, Phys. Rev. B**36** (1987) 4039

[41] D. Dijkkamp, T. Venkatesan, X.D. Wu, S.A. Shaheen, N. Jisrawi, Y.H. Min-Lee, W.L. McLean and M. Croft, Appl. Phys. Lett. **51** (1987) 619

[42] K. Koinuma, T. Hashimoto, T. Nakamura, K. Kishio, K. Kitazawa, and K. Fueki, Japanese J. of Appl. Phys. **26** (1987) 2761

[43] J. Geerk, H.C. Li, G. Linker, O. Meyer, C. Politis, F. Ratzel, R. Smithey, B. Strehlau, X.X. Xi and G.C. Xiong, Proc. 8th Int. Symp. on Plasma Chemicals, Tokyo 1987, eds. K. Akashi and A. Kinbara, p. 2349.

[44] B. Oh, M. Naito, S. Arnason, P. Rosenthal, R. Barton, M.R. Beasley, T.H. Geballe, R.H. Hammond and A. Kapitulnik, Appl. Phys. Lett. **51** (1987) 852

[45] H.C. Li, G. Linker, F. Ratzel, R. Smithey, and J. Geerk, Appl. Phys. Lett. **52** (1988) 1098

[46] X.X. Xi, H.C. Li, J. Geerk, G. Linker, O. Meyer, B. Obst, F. Ratzel, R. Smithey, and F. Weschenfelder, Physica C**153-155** (1988) 794;

[46a] X.X. Xi, G. Linker, O. Meyer, E. Nold, B. Obst, F. Ratzel, R. Smithey, B. Strehlau, F. Weschenfelder, J. Geerk, Z. Phys. B - Condensed Matter **74** (1989) 13

[47] W.K. Chu, J.W. Mayer, and M.A. Nicolet, Backscattering Spectroscopy, Academic Press, New York, 1978

[48] L.C. Feldman, J.W. Mayer and S.T. Picraux, Materials Analysis by Ion Channeling (Academic Press, New York, 1982).

[49] O. Meyer, H. Mann and G. Linker, Appl. Phys. Lett. **20** (1972) 259

[50] O. Meyer, F. Weschenfelder, J. Geerk, H.C. Li, and G.C. Xiong, Phys. Rev. B**37** (1988) 97, Nucl. Instr. and Meth. B (1988)

[50a] O. Meyer, F. Weschenfelder, X.X. Xi, G.C. Xiong, G. Linker, J. Geerk, Nucl. Instr. and Meth. B **35** (1988) 292

[51] G. Linker, X.X. Xi, O. Meyer, Q. Li, J. Geerk, Solid State Comm. **69** (1989) 249

[52] M.A. Beno, L. Soderholm, D.W. Capone II, D.G. Hinks, J.D. Jorgensen, J.D. Grace, I.K. Schuller, C.U. Serge and K. Zang, Appl. Phys. Lett. **51** (1987) 57

[53] K.B. Winterbon, Ion Implantation Range and Energy Deposition Distribution, Vol. **2**, Plenum, N.Y. (1975)

[54] J.F. Ziegler (ed.), The Stopping and Ranges of Ions in Matter, Vol. **1-6**, Pergamon Press (1980)

[55] J.P. Biersack, L.G. Haggmark, Nucl. Instr. and Meth. **174** (1980) 257

[56] J. Lindhard, M. Scharff, H.E. Schiott, Mat. Fys. Medd. ***33*** (1963) no. 14

[57] G.H. Kinchin, R.S. Pease, Rep. Progr. Phys. **18** (1955) 1

[58] T. Diaz de la Rubia, R.S. Averback, R. Benedek and W.E. King, Phys. Rev. Lett. **59** (1987) 1930

[59] F. Seitz and J.S. Koehler in Solid State Physics, F. Seitz and D. Turnbull (eds.), Academic N.Y. (1956) Vol. 2

[60] M.T. Robinson and I.M. Torrens, Phys.Rev. B**9** (1974) 5008

[61] A.R. Sweedler, D.E. Cox and S. Moehlecke , J. Nucl. Mat. **72** (1978) 50

[62] J. Remmel et al., to be published

[63] G. Hertel, A. Adrian, J. Bieger, C. Nölscher, L. Söldner, G. Saemann-Ischenko, Phys. Rev. B**27** (1983) 212

[64] J. Pflüger, O. Meyer, Solid State Commun. **32** (1979) 1143

[65] O. Meyer, G. Linker, J. Low Temp. Phys. **38** (1980) 747

[66] N. Kobayashi, R. Kaufmann, G. Linker, J. Nucl. Mat. **133/134** (1985) 732

[67] V. Jung, LT17, U. Eckern, A. Schmid, W. Weber, H. Wühl (eds.) North Holland, Amsterdam (1984) p. 109

[68] B. Egner et al., to be published

[69] P.P. Freitas, T.S. Plaskett, Phys. Rev. B**37** (1987) 3657

[70] A.D. Marwick, C.R. Guarnieri and J.M. Manoyan, Appl. Phys. Lett. **53** (1988) 2713

[71] (a) A. White (b) A.D. Marwick and G. Clark, private communication

[72] P.W. Anderson, Phys. Rev. **109** (1958) 1492

[73] M.A. Kirk, M.C. Baker, J.Z. Liu, D.J. Lam, H.W. Weber, Materials Research Soc. Meeting, Boston (1987)

[74] Y. Matsui, E. Takayama,-Muromachi, K. Kato, Jap. J. of Appl. Phys. **26** (1987) L1183

[75] G.J. Clark, A.D. Marwick , F. Legoues, R.B. Laibowitz, R. Koch, P. Madakson, Nucl. Instr. and Meth. B**32** (1988) 405

[76] R. Kaufmann, G. Linker and O. Meyer, Nucl. Instr. and Meth. **191** (1981) 532

[77] R. Kaufmann, G. Linker and O . Meyer, Nucl. Instr. and Meth. **218** (1983) 647

[78] F Weschenfelder, et al., to be published

[79] O. Meyer in Treatise on Materials Science and Technology, Vol. 18, Ion Implantation J.K. Hirvonen ed., Academic press, N.Y. 1980, p. 415

[80] B. Stritzker in Advances in Superconductivity, B. Deaver and J. Ruvals (eds.) Plenum Publishing Corporation, 1983

[81] B. Rauschenbach and K. Hohmuth, 6th Int. Conf. on Ion Beam Modification of Materials, June 88, Tokyo, Japan, to be published in Nucl. Instr. and Meth. B

[81a] B. Rauschenbach and K. Hohmuth, Z. Phys. B - Condensed Matter **74** (1989) 155

[82] Z.L. Liau and J.W. Mayer in Treatise on Materials Science and Technology, Vol. 18, Ion Implantation , J.K. Hirvonen ed., Academic Press, N.Y. 1980

[83] A.E. White, K.T. Short, D.C. Dynes, A.F.J. Levi, M. Anzlowar, K.W. Baldwin, P.A. Polakos, T.A. Fulton, L.N. Dunkleberger, Appl. Phys. Lett. **53** (1988) 1010

[84] R.H. Koch, C.P. Umbach, G.J. Clark P. Chaudhari, R.B. Laibowitz, Appl. Phys. Lett. **51** (1987) 200